ELSEVIER

Journal of Hydrology 262 (2002) 145–164

Journal of Hydrology

www.elsevier.com/locate/jhydrol

Snow processes in a forest clearing and in a coniferous forest

H. Koivusalo*, T. Kokkonen

Laboratory of Water Resources, Helsinki University of Technology, P.O. Box 5200, FIN-02015 HUT, Finland

Received 16 November 2000; revised 23 January 2002; accepted 14 February 2002

Abstract

An energy balance approach is applied to simulate snow accumulation and melt in a forest clearing and in a coniferous forest. The study site is located in southern Finland (60.1°N) where the winters are mild considering the high latitude. For forest simulations the snow model is coupled with a procedure, which accounts for the effects of the canopy on the driving meteorological variables of the snow model. Model results are first validated against measured values of snow water equivalent and snow temperature in a forested site and in an adjacent clearing. Subsequently differences in snow accumulation, snowmelt, and energy components contributing to snowmelt in open and forested conditions are studied. Effect of the canopy on snow mass balance on the ground can be seen as higher accumulation and more intense snowmelt in the open. Due to these counteracting processes the results show little difference in the annual maximum of the snow water equivalent between the clearing and the forest. The model results suggest that in mid-winter the main source of energy for snowmelt is sensible heat in the open, whereas both sensible heat and net radiation contribute equally to snowmelt in the forest. Solar radiation intensity increases towards the spring, which causes net radiation to become dominant in both sites.

Keywords: Snow; Melt; Forest; Energy fluxes; Mathematical models

1. Introduction

In high latitudes, snow accumulation and melt have a significant influence on hydrological processes. Precipitation stored in the snowpack over the winter is released in a relatively short period during snowmelt in spring, which typically gives rise to annual maximum streamflows. In the boreal region, a large fraction of the area is covered with forests where the influence of the canopy on snow processes is significant.

A number of snow models with varying complexity and data requirements are available for simulation of snow processes. The temperature-index approach is the simplest way to approximate the amount of energy available for snowmelt and requires only precipitation and air temperature as input data. When records of standard meteorological data (air temperature, precipitation, radiation components, relative humidity, wind speed) exist more complex models simulating the energy balance of snow can be applied. All these models have a similar boundary condition at the snow surface where the sum of upward and downward fluxes of energy results in change of snowpack temperature, snowmelt, or freezing of liquid water retained in the snow. Models have differences in description of the internal processes; some models consider the snowpack as a single bulk layer (Ohta, 1994; Price and Dunne, 1976; Tarboton et al., 1995), whereas others are more detailed in dividing the snowpack into multiple horizontal layers (Anderson,

* Corresponding author. Tel.: +358-9-451-3837; fax: +358-9-451-3836.

E-mail address: harri.koivusalo@hut.fi (H. Koivusalo).

0022-1694/02/$ - see front matter
PII: S0022-1694(02)00031-8

1976; Illangasekare et al., 1990; Jordan, 1991; Tuteja and Cunnane, 1997).

Data for temperature-index models are relatively widely available, which explains why they are popular in operational models for streamflow forecasting (Kustas et al., 1994; Kuusisto, 1984; Vehviläinen, 1992). The temperature-index approach is less applicable when separation of snow surface energy fluxes and prediction of the snow surface temperature are important, which is often the case when hydrological models are linked with atmospheric models (Marshall et al., 1999). More physically based approaches may also be called for when hydrological impacts of land-use changes, such as logging, are assessed (Lundberg, 1996).

Snow energy balance models have typically been designed to operate in open areas. Unforested areas exhibit energy exchange with the atmosphere that is radically different from the continuous forested areas (Harding and Pomeroy, 1996), and thence the application of these models in forested areas requires the influence of the canopy on the energy flux components to be taken into account. In several studies conducted in boreal region, net radiation has been found to increase in importance with respect to turbulent fluxes when a forest canopy is present (Link and Marks, 1999; Pomeroy and Dion, 1996; Price and Dunne, 1976; Woo and Giesbrecht, 2000).

Hardy et al. (1997, 1998) and Davis et al. (1997) studied spring snowmelt dynamics beneath deciduous and coniferous forest stands in Saskatchewan, Canada. They coupled a multi-layer snow energy balance model SNTHERM that has been demonstrated to perform well in open environments (Jordan, 1991) with a radiation transfer model, which accounted for the shading effect of the canopy. Woo and Giesbrecht (2000) and Giesbrecht and Woo (2000) considered spring snowmelt in a subarctic site in Yukon Territory, Canada, and accounted for the effect of canopy both at single tree and forest scales. All these studies have in common the fact that they concentrate on periods of little or no precipitation in the spring melt season and thus avoid the need to consider the effects of interception. Interception and sublimation of snow have been reported to result in substantial decrease in net precipitation in dense forests (Lundberg, 1993; Lundberg et al., 1998; Nakai et al., 1999; Pomeroy et al., 1998) and they have to be taken into account when snow processes are described over the entire winter season. Wigmosta et al. (1994) embedded into a hydrological model a soil–vegetation–atmosphere transfer scheme accounting for interception and the effect of canopy on radiative and turbulent fluxes and assessed their results against measured snow water equivalent and streamflow. Long-term snow accumulation–melt simulations considering other than only snow water equivalent and streamflow data in model calibration and validation have started to emerge (Storck, 2000), but are still limited in number.

In the present study, snow accumulation and melt are simulated over four winters in two adjacent sites of which one is clearing and the other one is covered with a mature coniferous forest. Snow modelling is based on an energy balance scheme that is coupled with a procedure accounting for interception and effects of the canopy on the radiative and turbulent energy fluxes. The objectives of this study are (1) to assess the model performance in terms of reproduction of measured snow water equivalent, snow temperature, and throughfall, (2) to compare the dynamics of the snow water equivalent in the open and in the forest, (3) to compare the snow surface energy fluxes in the open and in the forest, and (4) to identify the components of energy contributing to snowmelt in the open and in the forest in mid-winter and spring conditions. Sensitivity of the model simulations to parameterisation of the canopy procedure is also explored.

Climatic conditions in the present study area in southern Finland are more temperate than those in North American and Siberian regions having as northerly a location. Due to the effects of the Gulf Stream, winters are relatively mild and snowmelt may occur in mid-winder conditions when intensity of the solar radiation is insignificant. The role of different energy sources giving rise to snowmelt in such conditions has not adequately been addressed and this study attempts to add to this knowledge.

2. Site description and data

Snow, runoff and meteorological measurements were carried out during 1996–2000 in a forested catchment (Rudbäck, 18 ha) and in an adjacent clear-cut area (about 3 ha) in Siuntio, southern

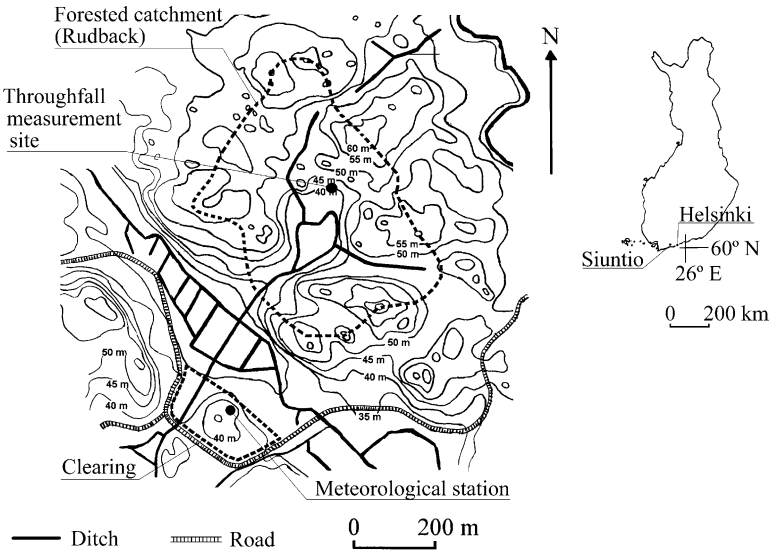

Fig. 1. Location of measurement sites in Siuntio, southern Finland.

Finland (Fig. 1). The Rudbäck catchment is one of the small research basins of the Finnish Environment Institute. The elevation ranges from 34 to 65 m. The catchment is covered by a mature forest stand dominated by Norway Spruce. The clearing has a few pine trees left for seeding and small spruces planted after the harvest. Bedrock is exposed on the hilltops and soils are composed of silty and sandy moraines with an average depth of 1–2 m to bedrock. More details on the site information are published in Lepistö (1994) and Lepistö and Kivinen (1997).

The climate is temperate with cold, wet winters, and precipitation is typically of a relatively low intensity. Mean annual precipitation (uncorrected) during 1991–1996 was 700 mm, which includes 15–25% of snowfall.

A matrix of 12 snow sticks was set up in the clearing, and a total of 22 sticks were placed in the forest to manually measure snow depth on the ground. Water equivalent of snow was measured at three points in both open and forested sites by weighing cylindrical snow samples. Micrometeorological variables at a height of 2 m above the ground surface were recorded in the clearing and in the forest below the canopy to provide input for the snow energy balance model. Half-hourly data include air temperature, relative humidity, wind speed, downward and reflected short-wave radiation in both sites, and precipitation in the open. Accumulated throughfall in the forest was measured manually at six points approximately once a week. Downward long-wave radiation was measured in the open until January 1999 and then the sensor was moved below the forest canopy. Additional temperature measurements were recorded at depths of 0.5, 0.3 and 0.1 m below the soil surface, and at heights of 0.1, 0.3 and 0.5 m above the ground in the forest. Similarly, in the open temperature measurements were recorded at 0.2 m intervals above and below the soil surface (from −0.3 to +0.3 m). In winter 1998–1999, the state of the canopy interception storage was visually observed approximately once a week. The state was described as (0) dry canopy, (1) wet canopy, (2) little snow captured in the canopy, (3) some snow captured in the canopy, and (4) much snow captured in the canopy.

The meteorological data were checked and edited to provide continuous hourly input for snow modelling. Air temperature was compared against manually measured readings to correct for a systematic bias. Relative humidity was scaled not to exceed 100%. Measured upward and downward short-wave radiation data were used to determine whether the radiation sensors pointing upwards were covered with snow. During periods of the sensors being snow-covered, the downward short-wave radiation was estimated using the measured upward short-wave radiation and an estimate of the new snow albedo of 0.85, and the downward long-wave radiation values were estimated

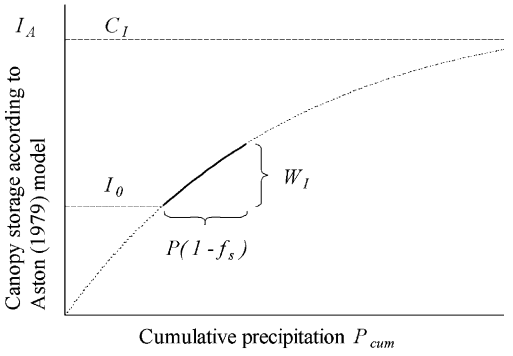

Fig. 2. Determination of the depth of intercepted water (W_I) during a single time-step. P is the depth of precipitation during a time-step, f_s is the sky-view fraction, C_I is the interception capacity, and I_0 is the canopy storage in the beginning of the computation time-step.

using the procedure suggested by Satterlund (1979). An estimate of cloudiness required in the Satterlund (1979) method was derived from the ratio of the measured short-wave radiation and the simulated clear-sky radiation.

Operation of the anemometers was occasionally hampered by intensive snowfalls, and wind speed was not measured in the forest between October 21, 1998 and January 25, 1999. When observed data from one of the two stations (forest or open) were not available, the missing values of wind speed were estimated from the existing records by multiplication with a scaling factor. The factor was selected according to the average ratio (0.21) between the wintertime wind speed in the forest and in the open.

Precipitation in the open was corrected using the procedure recommended for the Finnish H&H-90 measurement gauge in Førland et al. (1996). Six manually operated precipitation gauges in the forest, accumulated throughfall between the field visits. The average of the six gauge readings was assumed to represent the cumulative net precipitation in the forest. Stemflow was assumed negligible.

3. Methods

3.1. Canopy model

The canopy model largely follows the method given in Wigmosta et al. (1994), but the computation of overstorey interception has been modified and interception in the understorey vegetation has been ignored. The form of precipitation is determined on the basis of the air temperature. Below temperature T_l precipitation falls as snow and above temperature T_h as rain. Between T_l and T_h the proportion of snowfall (and rain) is a linear function of the air temperature. The canopy temperature is assumed to be equal to the air temperature. The share of precipitation falling between the trees is computed as a product of the total precipitation P and the sky-view fraction f_s. The remaining precipitation, i.e. $(1-f_s)P$, can be intercepted in the canopy and it forms the input to the interception procedure.

Calder (1990) notes that the maximum canopy storage is approached in a gradual manner and is only reached after accumulation of a considerably greater depth of rainfall than the capacity value. Aston (1979) has formulated this relationship mathematically as

$$I_A = C_I(1 - e^{-k_I P_{cum}/C_I}), \quad (1)$$

where I_A is the canopy storage in Aston's model, C_I is the interception capacity, k_I is a model parameter, and P_{cum} is the cumulative precipitation. This approach was originally proposed in the context of a single storm event assuming that the canopy storage is empty in the beginning of the event and evaporative losses need not to be accounted for. In the present model, the Aston relationship (Eq. (1)) is extended to simulate interception through multiple storm events with accountancy for interception evaporation. Computation of interception for snow and rain is carried out in an identical manner except for that C_I is higher for interception of snow (C_{IS}) than for interception of rain (C_{IW}).

Fig. 2 depicts in graphical terms how the depth of intercepted water during a time-step, W_I, is determined. In mathematical terms

$$W_I = (C_I - I_0) - (C_I - I_0)e^{-k_I(1-f_s)P/C_I}, \quad (2)$$

where I_0 is the canopy storage in the beginning of the computation time-step. Now the change in the canopy storage during a computation time-step, ΔI, can be written as

$$\Delta I = W_I - E_I, \quad (3)$$

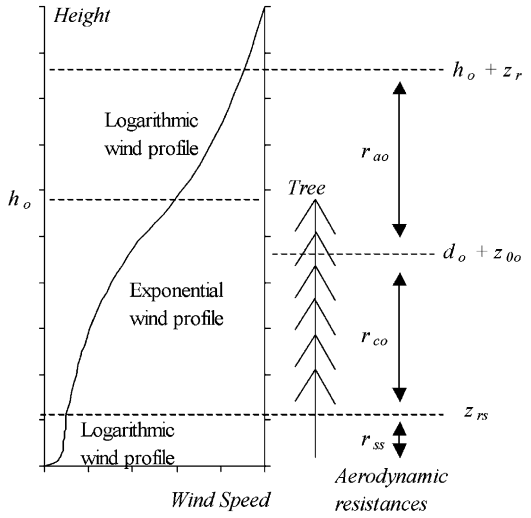

Fig. 3. Schematic of wind speed profile and aerodynamic resistances within and above canopy.

where E_I (Eq. (5)) is the depth of interception evaporation during a time-step.

To complete the description of the present interception model calculation of snow unloading is briefly discussed. When the air temperature increases above the freezing point and the canopy storage is greater than C_{IW} unloading of the intercepted snow (in excess of C_{IW}) occurs. Occurrence of snow unloading is checked in the beginning of the computation time step before the depth of intercepted water W_I is determined according to Eq. (2). Now throughfall P_T during a computation time-step can be written as

$$P_T = [(1 - f_s)P - W_I] + f_s P + U_S, \tag{4}$$

where U_S is the snow unloading during a computation time-step.

Interception evaporation out of the canopy storage is calculated using a combination equation of the Penman–Monteith type

$$E_I = \frac{\Delta R_{nc} + \rho_a c_p (e_s - e_a)/r_{ao}}{\lambda_v(\Delta + \gamma)}, \tag{5}$$

where Δ is the gradient of the saturated vapour pressure–temperature curve, R_{nc} is the net radiation in the canopy, ρ_a is the air density, c_p is the specific heat of air, e_s is the saturation vapour pressure, e_a is the air vapour pressure, r_{ao} is the aerodynamic resistance to vapour transport, λ_v is the latent heat of vaporisation, and γ is the psychrometric constant. Sublimation of snow in the temperatures below 0 °C is calculated by substituting λ_v with the latent heat of sublimation λ_s and adjusting the psychrometric constant by λ_v/λ_s in Eq. (5). Condensation into canopy is not allowed.

The aerodynamic resistance is calculated according to the eddy diffusion theory assuming equal resistances to transfer of heat, vapour and momentum. Although this assumption is known not to be strictly valid (Brutsaert, 1982; Male and Granger, 1981), it is commonly used in a hydrological context (Calder, 1990; Lundberg et al., 1998; Lundberg and Halldin, 1994; Wigmosta et al., 1994). The wind speed is assumed logarithmic above the canopy, exponential within the canopy, and logarithmic above the snowpack on the ground (Fig. 3). Aerodynamic resistance r_{ao} is computed by integrating the reciprocal of the eddy diffusion coefficient over the range from $d_o + z_{0o}$ to z_r (Dolman, 1993)

$$r_{ao} = \frac{1}{k^2 u_r} \ln\left(\frac{z_r - d_o}{z_{0o}}\right) \ln\left(\frac{z_r - d_o}{h_o - d_o}\right) + \frac{h_o}{n K_h}\left[e^{n - n(z_{0o} + d_o)/h_o} - 1\right], \tag{6}$$

$$K_h = \frac{u_r k^2 (h_o - d_o)}{\ln\left(\frac{z_r - d_o}{z_{0o}}\right)}, \tag{7}$$

where k is the von Karman constant, u_r is the wind speed at the reference height z_r, d_o ($= 0.63 h_o$) is the zero-plane displacement height, z_{0o} ($= 0.13 h_o$) is the roughness length of the canopy, h_o is the vegetation height, n is an extinction coefficient, and K_h is the logarithmic diffusion coefficient at the top of the canopy. Calder (1990) and Lundberg and Halldin (1994) note that aerodynamic resistance for the sublimation of snow is an order of magnitude higher due to the smooth surface of the intercepted snow. To account for these effects r_{ao} is multiplied by a factor $f_r = 10$ (Lundberg et al., 1998) at temperatures less than 0 °C.

The net radiation absorbed by the canopy is calculated ignoring multiple reflections between canopy and snow surface, and it is given by

$$R_{nc} = R_s(1 - f_s)[1 - \alpha_c - \tau_c(1 - \alpha_s)] + (1 - f_s)(R_{ld} + R_{ls} - 2R_{lc}), \tag{8}$$

where R_s is the incoming short-wave radiation, α_c is the albedo of the canopy, τ_c is the transmittance through the canopy, and α_s is the albedo of the surface below the canopy (snow or ground), R_{ld} is the downward atmospheric long-wave radiation, R_{ls} is the upward long-wave radiation from the surface below the canopy, and R_{lc} is the long-wave radiation emitted by the canopy (upward and downward). The albedo of canopy and ground surfaces was taken equal to 0.18. The computation of the snow albedo is described in Section 3.2.

The long-wave radiation terms are calculated as a function of the substrate temperature T_c using the Stefan–Boltzmann law

$$R_{lc} = \varepsilon_c \sigma T_c^4, \tag{9}$$

where σ is the Stefan–Boltzmann constant, and ε_c is the emissivity which equals unity for a vegetation surface and 0.99 for a snow surface.

3.2. Energy fluxes above the snowpack

Energy fluxes are computed using estimated values of meteorological variables beneath the canopy. In the computations, canopy is assumed to have an effect on radiation components, throughfall, and wind speed, while air temperature and relative humidity are taken equal to the values above the canopy.

Turbulent fluxes of sensible and latent heat are given by

$$H = \left(\frac{\rho_a c_p}{r_{s^*}} + E_{H0} \right)(T_a - T_0), \tag{10}$$

and

$$\lambda E = \left(\frac{\lambda_s 0.622}{r_{s^*} R_d (T_a + 273.15)} + E_{E0} \right)[e_a - e_s], \tag{11}$$

where H is the sensible heat flux, λE is the latent heat flux, ρ_a is the air density, c_p is the heat capacity of air, E_{H0} is the windless convection coefficient for the sensible heat flux, T_a is the air temperature, T_0 is the snow surface temperature, r_{s^*} is the aerodynamic resistance, R_d is the dry gas constant, E_{E0} is the windless convection coefficient for the latent heat flux, e_a is the air vapour pressure, e_s is the saturation vapour pressure at the snow surface, and λ_s is the latent heat of sublimation of ice. When the snow surface temperature is 0 °C the latent heat of vaporisation of water, λ_v, is used in Eq. (11).

The effect of canopy on turbulent heat fluxes due to reduced wind speed is accounted for in computation of the aerodynamic resistance between the snow surface and the reference height above the canopy (Fig. 3). Wind speed is assumed to decrease exponentially within the canopy as assumed in earlier studies of canopy evapotranspiration (Choudhury and Monteith, 1988). The exponential wind profile is assumed to merge with a logarithmic wind profile above the snowpack at the height of z_{rs} (= 2 m).

The resistance r_s to the turbulent heat exchange above the snowpack is calculated from

$$r_s = r_{ao} + r_{co} + r_{ss}, \qquad \text{in the forest} \tag{12a}$$

$$r_s = r_{ss}, \qquad \text{in the open} \tag{12b}$$

where r_{ao} is the resistance from Eq. (6), r_{co} is the resistance within the canopy, r_{ss} is the resistance between the snow surface and the height z_{rs}. Resistances r_{co} and r_{ss} are given by

$$r_{co} = \frac{h_o e^n}{n K_h}[e^{-n z_{rs}/h_o} - e^{-n(d_o + z_{0o})/h_o}], \tag{13}$$

and

$$r_{ss} = \frac{\left[\ln\left(\frac{z_{rs} - d_s}{z_{0s}} \right) \right]^2}{u_{rs} k^2}, \tag{14}$$

where d_s is the depth of the snowpack, z_{0s} is the snow surface roughness length, and u_{rs} is the wind speed at z_{rs}. The correction for stable and unstable atmospheric conditions is calculated from (Choudhury and Monteith, 1988)

$$r_{s^*} = r_s/(1 - 5Ri)^2, \text{ stable } 0 < Ri \le Ri_{max}, \tag{15}$$

$$r_{s^*} = r_s/(1 - 5Ri)^{3/4}, \text{ unstable } Ri < 0, \tag{16}$$

$$Ri = \frac{g(T_a - T_0)(z_{rs} - d_s)}{u_{rs}^2[0.5(T_a + T_0) + 273.15]}, \tag{17}$$

where Ri is an estimate of the Richardson number, Ri_{max} is the upper limit of the Richardson number, and g is the acceleration due to gravity.

Jordan et al. (1999) suggested that the correction for stable atmospheric conditions might lead to

Table 1
Parameters of the snow and canopy models, and perturbations of parameters in the sensitivity analysis

Parameters studied in sensitivity analysis	Symbol	Value	Perturbation in sensitivity analysis
Interception parameter	k_I	0.39	± 10%
Maximum interception capacity for water	C_{IW}	0.008 m	± 10%
Maximum interception capacity for snow	C_{IS}	0.03 m	± 10%
Sky-view fraction	f_s	0.15	± 10%
Canopy albedo	α_c	0.18	± 10%
Transmittance	τ_c	0.0	+ 0.1
Extinction coefficient	n	1.9	± 10%
Height of vegetation	h_o	25 m	± 10%
Zero-plane displacement height	d_o	15.75 m	± 10%
Roughness length of the canopy	z_{0o}	3.25 m	± 10%
Multiplier of resistance in snow conditions	f_r	10	± 10%
Lower temperature limit for form of precipitation	T_l	0.0 °C	± 0.5 °C
Upper temperature limit for form of precipitation	T_h	2.0 °C	± 0.5 °C
Windless convection coefficient for sensible heat flux	E_{H0}	7.2 kJ/m^2/h	± 10%
Windless convection coefficient for latent heat flux	E_{E0}	0.0 kJ/Pa/h	+ 0.15 kJ/Pa/h
Other model parameters and some physical constants			
Emissivity of snow[a]	ε_s	0.99	
Emissivity of vegetation surface	ε_c	1.0	
Ideal gas constant for dry air	R_d	287 J/kg/°K	
von Karman constant	K	0.41	
Maximum limit for Richardson number	Ri_{max}	0.16	
Snow surface roughness length	z_{0s}	0.005 m	
Measurement height for meteorological data	z_{rs}	2.0 m	
Atmospheric pressure[a]	P_0	100.8 kPa	
Maximum water equivalent of upper snow layer[a]	SWE_{act}	0.02 m	
Saturated hydraulic conductivity of snow[a]	K_{sat}	20 m/h	
Liquid water holding capacity of snow[a]	L_c	0.05	
Specific heat of soil particles[a]	C_g	0.84 kJ/kg/°C	
Density of soil particles[a]	ρ_g	2650 kg/m^3	
Depth of soil layer[a]	D_g	0.8 m	
Soil porosity[a]	ϕ	0.5	
Soil water content[a]	w	0.45	
Freezing depression curve parameter[a]	d_g	1.5 °C	
Albedo of ground[a]	α_g	0.18	

[a] These parameters/constants are not found in Section 3, but their values are reported here for information (parameter definitions in Koivusalo et al. (2002)).

cessation of turbulent heat exchange and excessive cooling of the snow surface during cold periods with low wind speeds. In the present snow model an attempt is made to alleviate these problems by limiting value of the Richardson number and by allowing windless exchange of the sensible heat. The windless convection coefficient E_{H0} in Eq. (10) enables sensible heat transfer to occur even when wind speed is zero and thereby prevents surface temperature from falling to unrealistically low values in response to radiative losses. Jordan et al. (1999) suggested that the windless convection coefficient for latent heat, E_{E0}, had no similar effect and therefore it was set equal to zero. Values for windless exchange coefficients are given in Table 1.

In the presence of a canopy net radiation flux R_{ns} into the snowpack is given by

$$R_{ns} = R_s[\tau_c(1 - f_s) + f_s](1 - \alpha_s) + R_{lc}(1 - f_s) + R_{ld}f_s - R_{ls}, \quad (18a)$$

and in the open it is computed from

$$R_{ns} = R_s(1 - \alpha_s) + R_{ld} - R_{ls}. \quad (18b)$$

Wigmosta et al. (1994) applied separate functions for snow accumulation and melt seasons to describe the decrease in snow albedo as a function of time since the last snowfall. Calculation of snow albedo in the present study rests on these functions. Winters in southern Finland have typically several accumulation–melt cycles, and thus a subdivision of a winter into one accumulation and one melt season was deemed to be too coarse. Instead, accumulation and melt periods are separated on the basis of the air temperature, and each period is associated with a corresponding albedo decrease function. This albedo computation scheme can be formulated as

$$\alpha_s^{t+\Delta t} = \alpha_s^t + \Delta\alpha_s^t, \quad (19)$$

and

$$\Delta\alpha_s^t = \begin{cases} \alpha_0\left[0.94^{(t+\Delta t)^{0.58}} - 0.94^{t^{0.58}}\right], & T_a^t < 0\ ^\circ\mathrm{C} \\ \alpha_0\left[0.82^{(t+\Delta t)^{0.46}} - 0.82^{t^{0.46}}\right], & T_a^t \geq 0\ ^\circ\mathrm{C} \end{cases}, \quad (20)$$

where t is the time elapsed since the last snowfall (in days), α_0 is the albedo of new snow (0.85), $\Delta\alpha_s^t$ is the change of albedo from t to $t + \Delta t$, and T_a^t is the air temperature at time t. The albedo is reset to α_0 after a snowfall event exceeding 2 mm (as water equivalent).

The advective heat flux Q_P from precipitation (or throughfall) is calculated as the energy needed to convert precipitation to ice phase at 0 °C. For example, rain-on-snow increases the liquid water mass of the snowpack and hence the heat content of the snowpack is increased by the energy which would be released if this rain was first cooled to 0 °C and then frozen.

3.3. Snow energy balance model

The snow model used in the current study has been described in detail in Koivusalo et al. (2002), and only a brief summary is given here. The model is one-dimensional and it simulates heat conduction through the snow into the soil, snowmelt, liquid water retention in snow, melt water discharge out of a snowpack, and compaction of snow. Time-series of water equivalent, depth, and temperature of snow are produced as an output. Computation procedures are based on the ideas from Tarboton et al. (1995) and Karvonen (1988). In the model, the snow–soil domain is split into two layers of snow and one of soil. Separation of the snow into two layers restricts the heat exchange with the atmosphere only to a part of the snowpack, and inclusion of the soil layer enables consideration of the ground freezing, where both aid in obtaining a realistic estimate of the snow surface and snowpack temperatures. The heat content of each layer is used to determine the average temperature and the liquid water content of a layer.

Energy balance at the snow–air interface is formulated as

$$M_0 + Q_0 = R_{ns} + H + \lambda E + Q_P, \quad (21)$$

where M_0 is the energy available to melt snow, Q_0 is the heat conduction to the top snow layer, R_{ns} is the net radiation at the snow surface, H is the sensible heat flux, λE is the latent heat flux, and Q_P is the advective heat flux from precipitation. Snow surface temperature is iterated from Eq. (21) by balancing the sum of right-hand terms with heat conduction Q_0 into the snow. When the snow surface temperature reaches 0 °C, all the remaining energy is used to melt snow. The term snowmelt refers to phase change of ice into water within the snowpack. Meltwater is stored within the snowpack until liquid water retention capacity is exceeded and water is discharged out of the snowpack.

Koivusalo et al. (2002) have successfully validated the performance of the snow model against field data of snow internal variables and surface fluxes measured in northern Finland, and against results of a multi-layer snow energy balance model SNTHERM (Jordan, 1991).

4. Results and discussion

4.1. Performance criteria

The model results are assessed in terms of two performance criteria. These are mean absolute error E_{ma} and bias B

$$E_{ma} = \frac{1}{N}\sum_{i=1}^{N}|\hat{x}_i - x_i|, \quad (22)$$

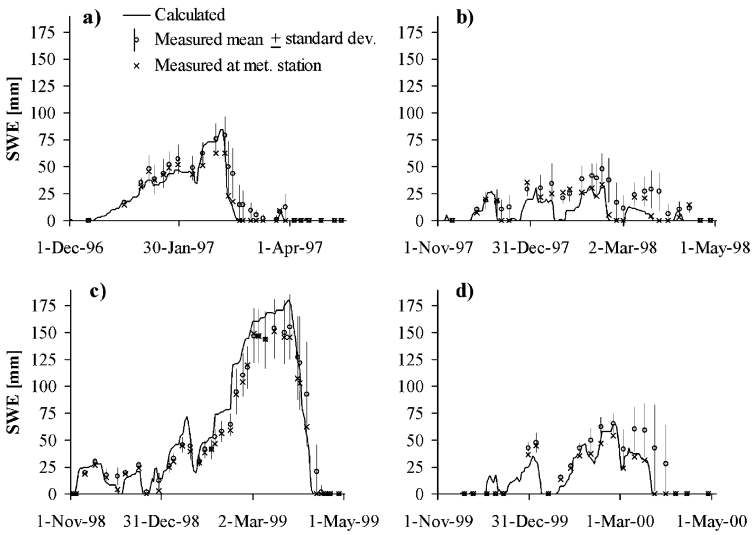

Fig. 4. Calculated water equivalent of snow (SWE), and measured SWE (mean ± standard deviation) in the open during four winters (a, b, c, d) from 1996 to 2000. Measured SWE at an observation site located next to the meteorological station is also shown.

$$B = \frac{1}{N}\sum_{i=1}^{N}(\hat{x}_i - x_i), \tag{23}$$

where N is the number of observations, $\hat{x}_i$ is a calculated value, and x_i is a measured value.

4.2. Clearing

Snow processes in the open are studied during four winters from 1996 to 2000.

The model simulates one-dimensional vertical processes at a point and does not take into account horizontal redistribution of mass or advection of energy. The model uses as input hourly data of precipitation, air temperature, relative humidity, wind speed, downward short-wave and long-wave radiation measured at a height of 2 m above ground. Parameters of the snow model (Table 1) are largely based on the values suggested for a snow energy balance model in Tarboton and Luce (1996). Soil parameters are taken as typical values characterising moraine soil. In addition, soil water content and thickness of the soil layer were adjusted by comparing measured and modelled soil temperatures. The modelling results are assessed against measured values of water equivalent and temperature of snow.

Fig. 4 shows the water equivalent of snow in the clearing for the whole study period. The four winters exhibit considerable differences in snow dynamics. Winter 1996–1997 had only one major accumulation–melt cycle. The warm spells in the middle of the winter, which are common along the southern coast of Finland, were not long enough to melt the entire snow cover at any of the observation points. Only little spread between minimum and maximum values of the water equivalent of snow was measured in the beginning of the winter, which is mainly due to relatively low wind speeds during snowfalls. Later the spatial variability of the water equivalent greatly increased as a result of higher wind speeds during snowfalls. These results suggest that in the clearing snow drift has a significant role in the spatial distribution of snow mass. A prominent feature of this winter is that the entire snowpack melted by the end of February. Thereafter, only minor snowfalls occurred and the ground remained snow free for most of the time.

The winter of 1997–1998 had several warm spells, which gave rise to temporary snowmelts and low values of maximum snow water equivalent. The spatial variability in snow water equivalent was higher than in the previous winter. This variability is a result of both snow drift and snowmelt. Snowmelt variability arises from spatial differences in radiative and turbulent energy flux components. For example, the aspect varies in the forest clearing and gives rise to differences in downward flux of short-wave radiation.

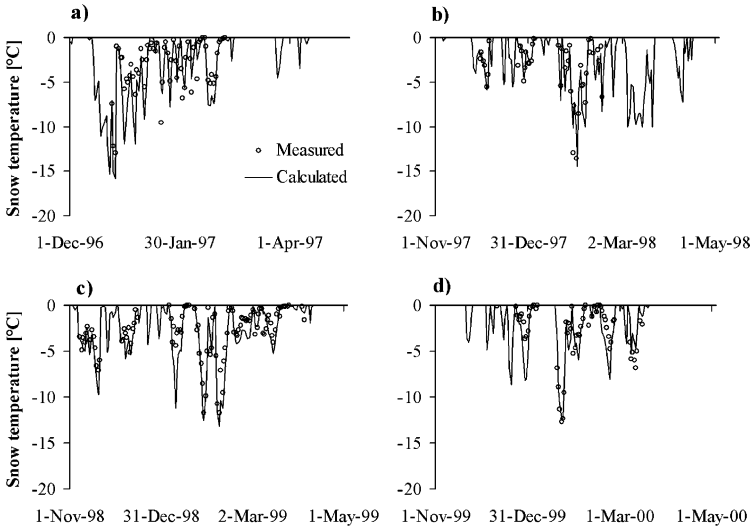

Fig. 5. Measured and modelled snowpack temperatures (daily averages) in the open for four winters (a, b, c, d) from 1996 to 2000. The calculated temperature is a weighted average of the snow temperatures in the two snow layers with the weights being equal to the layer depths.

In the beginning of the winter 1998–1999 snow accumulation and melt periods alternated until snowfalls in February lead to a build-up of a deep snowpack. The deep snow cover lasted until the final snowmelt from late March to mid April. The average snow water equivalent had a maximum value of 155 mm (Fig. 4), which corresponds to a return period of about 5 years (Kuusisto, 1984). The winter 1999–2000 was rather similar to the winter 1997–1998 having again warm spells in the middle of the winter.

In Fig. 4, the modelled snow water equivalent is compared against measured mean snow water equivalent. Assessment of the model performance is based on the rate of change in snow water equivalent between observations. Change in snow water equivalent ($SWE_{new} - SWE_{old}$) is considered to avoid propagation of the error from one period between observations to another. The mean absolute error for the entire study period, i.e. for all four winters, is 1.29 mm/d. When snow accumulation and melt periods are considered separately, the model errors for accumulation and melt are found not to originate from identical populations (Wilcoxon rank-sum test, risk level of 1%). Mean absolute errors for accumulation periods ($N = 55$) and melt periods ($N = 20$) are 0.88 and 2.38 mm/d, respectively, and biases are -0.11 and -1.78 mm/d. The results suggest that the model reproduces more accurately snow accumulation than snowmelt. The calculated biases indicate that the precipitation measurement has small systematic error, whereas snowmelt is overpredicted throughout the study period. The weather station was placed on a small ridge in the middle of the clearing in order to minimise the effects of shading and turbulence caused by the surrounding forest. With regard to snowmelt this exposed location, however, is not representative of the snowmelt conditions in the sheltered areas on the ridge sides, where many of the snow sticks were located. Fig. 4 also shows the measured water equivalent at an observation point located next to the meteorological station. Assessment of model results against these values yields mean absolute errors of 0.99 and 1.73 mm/d, and biases of -0.16 and -0.29 mm/d for accumulation and melt periods, respectively. The small absolute value of bias for melt periods indicates that now there is less systematic error in snowmelt predictions than when comparing against the mean snow water equivalent.

The readings of two temperature sensors at a height of 0.1 and 0.3 m above the ground were used to derive the snowpack temperature, which was taken as the average reading of the sensors located below the snow surface. The elevation of the surface was interpolated from snow depth measurements. The modelled temperature of the snowpack was calculated as a weighted average of the snow temperatures in the

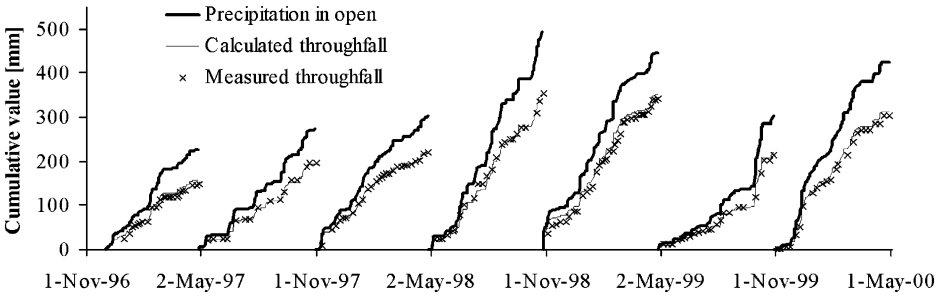

Fig. 6. Measured and calculated cumulative throughfall, and measured cumulative precipitation in the open for winter and summer seasons from 1996 to 2000.

two snow layers with the weights being equal to the layer depths. Fig. 5 shows the measured and modelled snowpack temperatures (daily average) for four winters from 1996 to 2000. The mean absolute error is 1.26 °C and bias is −0.61 °C. Large errors can occur when a temperature sensor actually measures the air temperature even though according to the interpolated snow depth it should reside within the snowpack.

4.3. Forest

Snow accumulation and melt on the ground below the forest canopy were modelled using the same parameterisation of the snow model as that used in the open. The effect of canopy on mass and energy fluxes was taken into account with an additional procedure, which requires as input the same meteorological variables as the snow model. Ideally, these variables ought to be measured above the canopy, but in this study the meteorological data measured in the open were assumed to be representative of the conditions at a height of 2 m above the canopy.

The canopy model was calibrated against meteorological data measured below the canopy. Parameter values resulting from calibration are listed in Table 1. A sky-view fraction was estimated by comparing the measured and calculated series of downward long-wave radiation beneath the canopy for a period from 10 January to 13 October 1999. For the entire period average daily long-wave radiation flux beneath the canopy was 30.2 MJ/m^2/d and the mean absolute error between measured and calculated daily values was 0.37 MJ/m^2/d. Comparison of measured and calculated series of downward short-wave radiation beneath the canopy results in a negligibly small value of transmittance τ_c. The measured average of daily short-wave radiation beneath the canopy for a period from 1 December 1996 to 13 October 1999 was 1.3 MJ/m^2/d and the mean absolute error was 0.33 MJ/m^2/d. The parameter n in Eqs. (6) and (13) was estimated by comparing the measured and calculated series of wind speed beneath the canopy for a period from 1 December 1996 to 13 October 1999. The mean wind speed for the entire period was 0.20 m/s and the mean absolute error between measured and calculated daily averages was 0.07 m/s.

Fig. 6 shows the measured and calculated cumulative throughfall, and measured cumulative precipitation in the open separately for winter and summer seasons. Winter season starts in November and ends in April, and summer season covers the period from May to October. The interception parameters (C_{IS}, C_{IW}, k_I) were calibrated against measured throughfall for a period from 1 December 1996 to 30 April 1999. A period from 1 May 1999 to 28 April 2000 was used for validation. Mean absolute errors were 0.31 and 0.16 mm/d and biases were 0.02 and 0.01 mm/d for calibration and validation periods, respectively. There is little difference between interception losses in summer and winter seasons. The average interception losses for summer and winter seasons are 29 and 26%, respectively. Interception evaporation during the winter, when the zenith angle of the sun is wide and net radiation is of low intensity, is mainly explained by advection of energy due to turbulence within and above the forest canopy. Considerable wintertime interception has also been reported in Nakai et al. (1999), Pomeroy et al. (1998) and Lundberg et al. (1998).

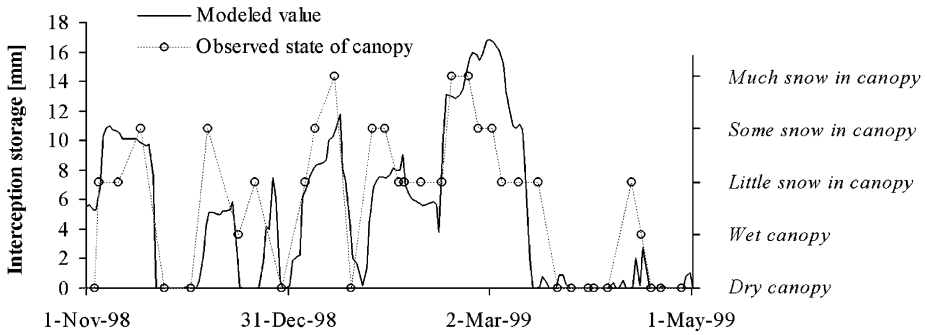

Fig. 7. Modelled amount of water or snow captured in the canopy storage and visual observations of the state of the canopy interception storage for winter 1998–1999.

In Fig. 7, the modelled amount of water or snow captured in the canopy storage is presented along with the visual observations on the state of the canopy interception storage for winter 1998–1999. According to both model results and visual observations the canopy dries completely several times during the winter. In the middle of February, when the model calculated maximum values for the snow intercepted in the canopy, the observed snow load in the canopy was very high. Severe snowstorms accompanied with formation of rime in the trees caused branches and even trunks to crack.

The water equivalent of snow on the ground below the canopy is shown in Fig. 8 for the whole study period. Similarly to the open, the spatial variability in the measured water equivalent is high as indicated by the large standard deviation. In the forest this variability is mostly a result of spatial differences in throughfall and snowmelt. Snow drift has little impact, because wind speeds beneath the canopy are low.

Performance of the snow model is again assessed against the rate of change in snow water equivalent

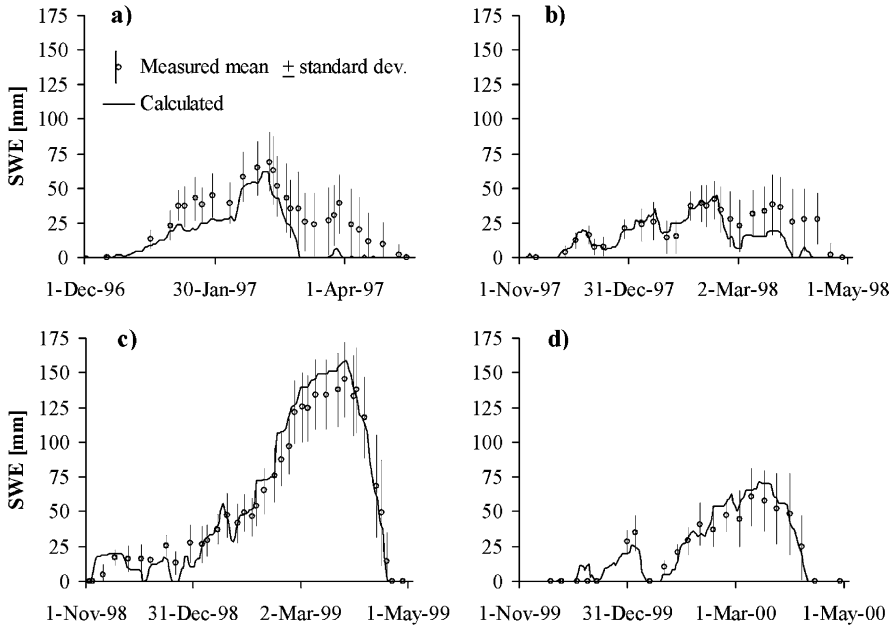

Fig. 8. Calculated water equivalent of snow (SWE), and measured SWE (mean ± standard deviation) in the forest during four winters (a, b, c, d) from 1996 to 2000.

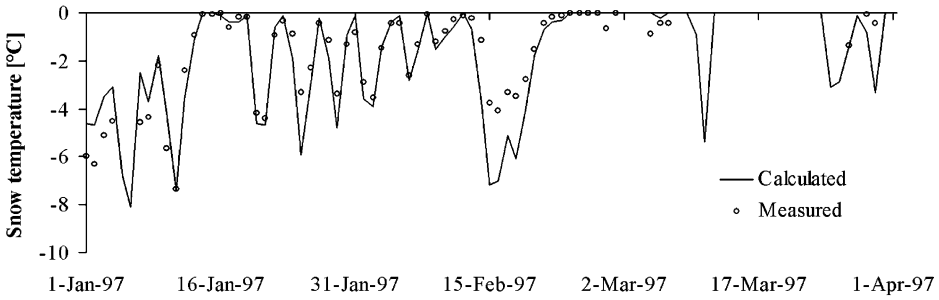

Fig. 9. Measured and calculated snow temperatures (daily averages) in the forest for a period from January to March, 1997. The calculated temperature is a weighted average of the snow temperatures in the two snow layers with the weights being equal to the layer depths.

between observations. The mean absolute error for the entire study period is 1.12 mm/d. Mean absolute errors for accumulation periods and melt periods are 1.03 and 1.26 mm/d, respectively, and biases are −0.29 and −0.03 mm/d. In terms of the performance criteria the snow model beneath the canopy yields similar results compared with those obtained in the clearing. Snowmelt is clearly overpredicted in early March 1997. The modelled snow water equivalent is sensitive to the air temperature; a good fit for spring 1997 would be easily achieved by subtracting less than 1 °C from the measured temperatures. Such data manipulation was not considered to be appropriate, although it is possible that even after correction there still are errors of that magnitude in the temperature data.

The measured and calculated snow temperatures (daily average) in the forest are plotted for a period from January to March, 1997, in Fig. 9. Due to problems with the instrumentation there are no reliable measurements available for any other period. The mean absolute error and bias for the period are 0.82 and −0.12 °C, respectively. Because depth of the snow in that winter never reached the level of the second temperature censor at a height of 0.3 m, the measured temperature was always based on only one temperature reading at a height of 0.1 m. Since the temperature gradient within a snowpack can be very steep during cold periods, just one reading does not give a good estimate of the average snowpack temperature. This is one possible explanation for the poor model fit in the middle of February when the air temperature dropped below −10 °C and the measured snow depth reached 0.25–0.29 m leaving the single temperature reading at the bottom third of the snowpack. This issue was studied more closely by comparing the measurements against the calculated temperature in the lower one of the two snow layers present in the model. Throughout the period from 12 to 25 February the single temperature sensor resided within the bottom snow layer. Mean absolute error for the average snowpack temperature for that period was 1.15 °C, whereas comparison of the measured temperature against the calculated bottom layer temperature yielded a considerably smaller error of 0.36 °C.

4.4. Comparison between clearing and forest

Here the differences in snow processes with and without forest canopy are discussed. The approach taken is to compare modelled snow water equivalent, cumulative snowmelt, and energy fluxes above the snow surface in the open and in the forest. Recall that the same set of meteorological input data have been used in running the snow model in the open, and the coupled canopy and snow model in the forest. The objective is to isolate the effect of canopy on snow processes from other factors, such as snow drift and spatial differences in snowmelt. Hence the modelled snow masses are used in the comparison instead of the measured averages, which are affected by the spatial differences in snowmelt especially in the clearing (see Section 4.2). Furthermore, there are no measured data on all energy flux components of interest.

The modelled snow water equivalent and cumulative snowmelt in the open and in the forest are presented for the entire study period in Fig. 10. The cumulative snowmelt includes rainfall in periods when there is no snow on the ground. Throughout

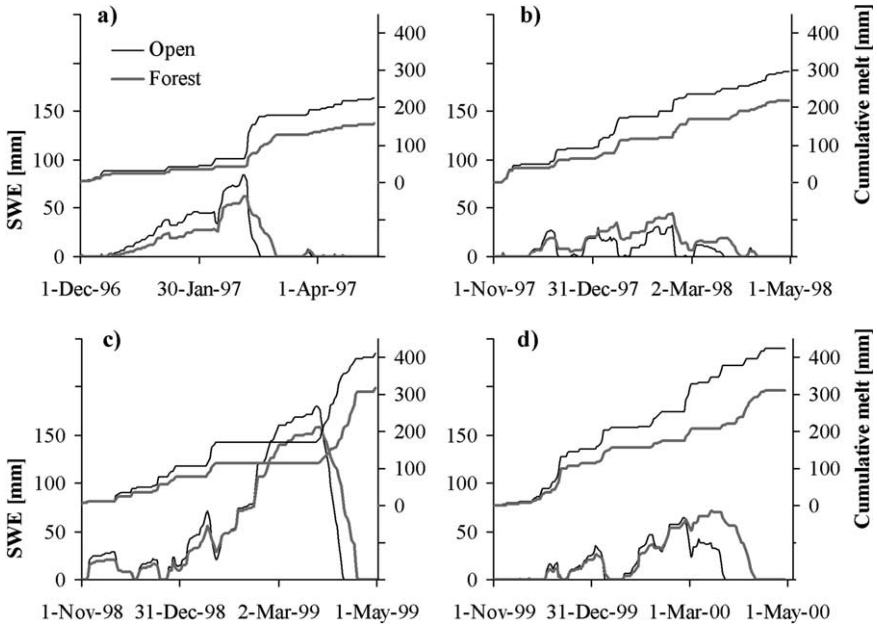

Fig. 10. Modelled snow water equivalent (SWE) and cumulative snowmelt in the open and in the forest during four winters (a, b, c, d) from 1996 to 2000. The cumulative snowmelt (shown on top of SWE) includes rainfall in periods when there is no snow on the ground.

the winter snow water equivalent may be greater either in the open or below the canopy depending on meteorological conditions. Because of higher net precipitation in the open, snowfall events, such as those in February 1999, cause the water equivalent to increase more rapidly in the open than in the forest. On the other hand, the greater intensity of snowmelt in the open causes the water equivalent to decrease faster than in the forest. The result of higher accumulation and more intense snowmelt in the open relative to the forest is qualitatively similar to the findings of Troendle (1983) and Troendle and King (1987). During a sequence of warm spells snow mass in the open falls below that in the forest (see e.g. December 1997 to January 1998). The maximum value of the average snow water equivalent in each winter is nearly equal in the forest and in the open. Even though the clearing receives more precipitation than the forest, the more intense snowmelt in the clearing is capable of compensating for this.

Fig. 11 shows cumulative energy fluxes above snow surface in the open and in the forest. Note that the fluxes are accumulated only when there is snow on the ground. Positive flux is directed towards the snow. The most prominent differences can be seen in net radiation and sensible heat fluxes. Net all-wave radiation in the open is dominated by an upward net flux of long-wave radiation until in spring intensity of solar radiation increases and reverses the net radiation flux to point downwards. In mid-winter net radiation is much less negative in the forest where the canopy significantly contributes to downward long-wave radiation. In spring, net radiation intensity is lower in the forest due to a canopy shading effect. The loss of radiative energy in the open results in an efficient cooling of the snow surface in mid-winter, which together with higher wind speeds gives rise to a much greater flux of sensible heat compared to that in the forest. The latent heat fluxes contribute only little to the total energy balances both in the open and in the forest.

The advective heat flux from precipitation as defined in Section 3.2, includes energy associated with phase change (freezing) in the case of rain, and temperature changes to bring the precipitation to the reference temperature (0 °C). The phase change energy is the largest component of the advective flux. During rain on snow events the energy associated with phase change does not actually go to generating melt. Rain on a cold snowpack freezes releasing

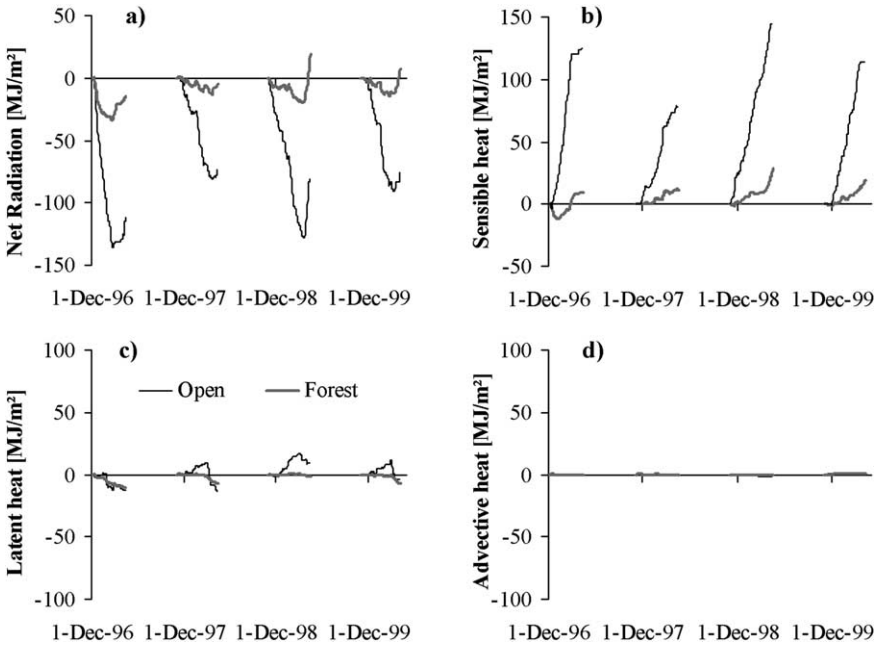

Fig. 11. Modelled cumulative fluxes of net radiation (a), sensible heat (b), latent heat (c), and advective heat associated with temperature change (d) above snow surface in the open and in the forest from 1996 to 2000. Positive flux is directed towards the snow.

energy to the snow and raising its temperature until the snowpack is isothermal (0 °C). Once this occurs rain does not freeze so the only energy that goes to melt snow is due to temperature changes. The rain water added does, however, mingle with melt water and contribute to melt outflow. In order to explore the importance of advective heat flux in generating snowmelt Fig. 11(d) shows only the advective heat component associated with temperature changes. From Fig. 11 it is clear that the advective heat flux contributes only little to snowmelt.

In Fig. 12 daily sums of net radiation, sensible heat, and latent heat are plotted for winter 1998–1999. In the open, snowmelt events in mid-winter occur when the weather is warm and cloudy. In such conditions snowmelt is mainly driven by sensible heat with latent heat flux occasionally having a significant contribution. Also, net radiation flux is only slightly negative or sometimes even positive. The increase in solar radiation intensity causes net radiation to become the most significant source of energy contributing to snowmelt in late spring. Unlike in the open, net radiation in the forest contributes significantly to snowmelt throughout the winter. In mid-winter peak values of net radiation arise from long-wave radiation emitted by the canopy and in spring from both short- and long-wave radiation. During melt events in mid-winter sensible heat flux is of the same magnitude as net radiation flux. Latent heat flux is insignificant throughout the winter. It is noteworthy, that wind speeds below the canopy are low and the contribution of the sensible heat flux to snowmelt is largely dependent on the selection of the windless convection coefficient (E_{H0} in Eq. (10)), whose value was adopted from Jordan (1992). Unlike the radiation components the computed turbulent heat fluxes have not been validated against measurements. Particularly in the forest, the modelled partitioning of the turbulent energy into sensible and latent heat fluxes is sensitive to the modelling choice of giving E_{H0} a nonzero value and setting E_{E0} to zero. As documented and cited earlier (see Section 3.2), this parameterisation was based on previous snow modelling studies.

The dominant role of net radiation in spring melt is consistent with earlier results from boreal forests (Link and Marks, 1999; Pomeroy and Dion, 1996; Price and Dunne, 1976). These studies do not address mid-winter snowmelt, since it rarely occurs in the

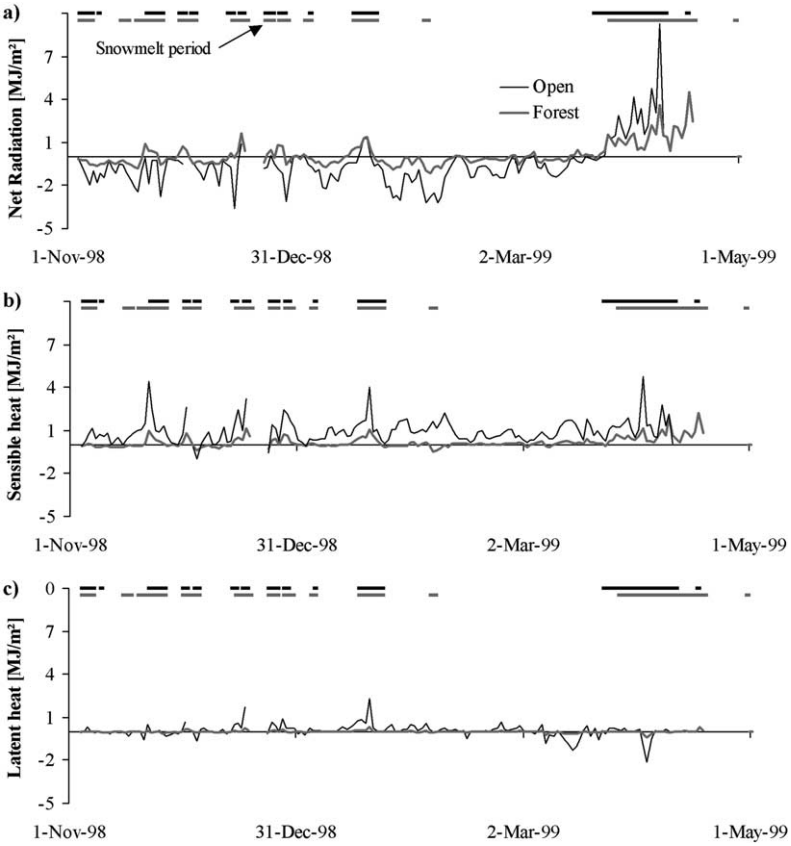

Fig. 12. Computed daily sums of net radiation (a), sensible heat (b), and latent heat (c) in the open and in the forest for winter 1998–1999. Fluxes are shown only when there is snow on the ground. Horizontal lines on top of the fluxes indicate periods when snowmelt occurred.

climatic conditions exhibited by their study sites. The mid-winter melt events occurring in the current study site are associated with warm, cloudy weather when both long-wave radiation and sensible heat flux contribute to snowmelt. As mentioned earlier, solar radiation intensity in the middle of the winter is insignificant.

4.5. Sensitivity of model results on canopy parameterisation

The effect of perturbing canopy model parameters on computed mean values of throughfall and snow water equivalent is studied here. Mean throughfall is computed omitting hours of no throughfall. Mean snow water equivalent is derived by averaging the results over all time-steps when snow is present. Table 1 lists perturbations of the studied parameters.

Fig. 13 shows the model sensitivity to parameter perturbations in terms of relative changes in mean throughfall and snow water equivalent. Throughfall is most sensitive to the sky-view fraction f_s, the interception parameter k_I, and all parameters (h_o, d_o, z_{0o}) in Eq. (6) determining the aerodynamic resistance. Throughfall is found to be much less sensitive to the parameters that influence computation of net radiation intensity within the canopy. This result is in line with the finding of Lundberg and Halldin (1994) who reported the estimation of interception evaporation to be very sensitive to the aerodynamic resistance. Snow water equivalent shows similar sensitivity to parameters k_I and f_s, to which throughfall was also found to be sensitive. In addition, it is very sensitive to threshold temperatures T_l and T_h, which determine the form of precipitation, and sensitive to the extinction coefficient n, which affects the turbulent heat fluxes.

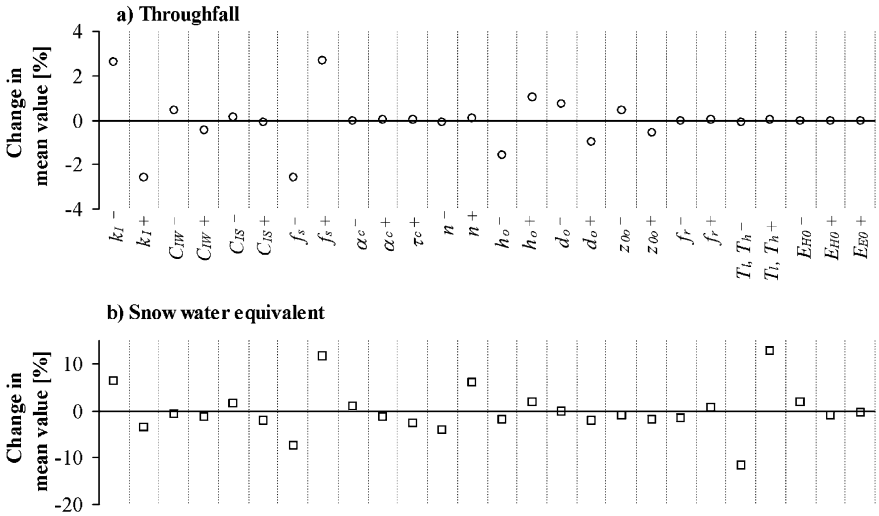

Fig. 13. Model sensitivity to parameter perturbations in terms of relative changes in mean throughfall (a) and snow water equivalent (b).

As seen in Section 4.4, snowmelt conditions in the study area are clearly different in mid-winter and springtime. Therefore, sensitivity of the computed surface energy fluxes contributing to snowmelt is studied separately for two snowmelt periods, of which one occurs in late January and the other one in early April, 1999. Fig. 14 shows absolute changes in energy components in response to parameter perturbations for the two melt periods. The same figure presents partition of the total energy into short- and long-wave radiation, sensible heat and latent heat fluxes, and advective heat flux from precipitation (Fig. 14(b) and (d)). Absolute changes are examined here in order not to accentuate large relative changes in fluxes of small intensity.

The mid-winter melt occurs during cloudy weather

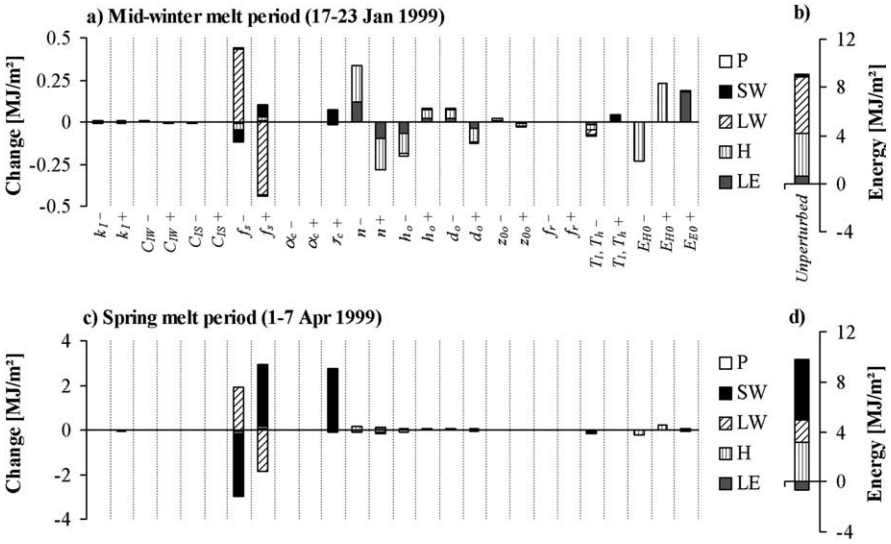

Fig. 14. Absolute changes in energy components in response to parameter perturbations during mid-winter melt period (a), partition of total energy into short- and long-wave radiation, sensible heat, latent heat, and advective heat associated with temperature change during mid-winter melt period (b), absolute changes in energy components during spring melt period (c), partition of total energy during spring melt period (d).

when primary sources of energy giving rise to snowmelt are long-wave radiation and sensible heat flux. In the springtime melt period short-wave radiation is the greatest contributor to snowmelt followed by sensible heat flux. In the mid-winter period changes in individual energy components resulting from parameter perturbations are less than 5% (relative to the total energy), whereas in the spring period changes close to 30% are seen. Perturbing the sky-view fraction f_s affects the role of long-wave radiation as a contributor to snowmelt in both periods, and the role of short-wave radiation in springtime. Contribution of short-wave radiation to spring melt is also influenced by perturbation of the transmittance τ_c. Largest changes in turbulent heat fluxes are due to perturbations in extinction coefficient n and windless exchange coefficients E_{H0} and E_{E0}, as seen in the mid-winter period plot. Sensitivity of the turbulent heat flux computation is similar for the spring period, but this effect is masked by much larger changes in the solar radiation component.

5. Conclusions

Assessment of model results from the open against measured mean snow water equivalent reveals that snow mass changes are simulated more accurately during periods of snow accumulation than during periods of snowmelt. Small bias (−0.11 mm/d) of the computed snow accumulation rate indicates that the precipitation measurement has little systematic error. When model results in the open were compared against observations next to the meteorological station, snowmelt was more accurately reproduced. This is due to different snowmelt conditions at the exposed location of the meteorological station when compared with the average conditions within the clearing. Ideally, if distributed meteorological data were available, the average snow mass should be computed using the distributed input data and averaging the model outputs.

A significant proportion of the precipitation was captured in the canopy both during summer and winter. The average interception evaporation was 26% for winter seasons, and 29% for summer seasons. There is little difference in cumulative interception in winter and summer, although radiation intensity in the winter is drastically lower. Interception during the winter is mainly explained by advection of energy due to turbulence within and above the forest canopy.

The effect of the canopy on snow mass balance on the ground can be seen as higher accumulation and more intense snowmelt in the open. As winters in the study site typically comprise several accumulation–melt cycles the snow water equivalent may be greater at any time either in the open or below the canopy. Also, there is little difference in the maximum values of the average snow water equivalent in each winter. When a warm spell is short enough to leave snow on the ground both in the open and in the forest, the cumulative snowmelt during one event is always higher in the open. As the maximum snow water equivalent prior to the spring melt is nearly equal in both sites, there is not much difference in the cumulative spring snowmelt. Melt is more rapid in the open leaving the ground free of snow when there is still snow melting in the forest. In conditions similar to the study site the impact of forest harvesting would be most clearly seen as increase of net precipitation and hence as increase of water volume contributing to streamflow over the winter season. However, the volume of spring runoff resulting from the final melt may not change.

The comparison of modelled energy fluxes above the snow surface revealed major differences in net radiation and sensible heat fluxes in the open and below the canopy. The contribution of canopy to long-wave radiation was clearly seen in mid-winter as smaller radiation losses in the forest. In spring the net radiation is of lower intensity in the forest due to a canopy shading effect on short-wave radiation. Sensible heat flux in the open is much greater than below the canopy. In mid-winter the main source of energy for snowmelt is sensible heat in the open, whereas both sensible heat and net radiation contribute equally to snowmelt in the forest. Solar radiation intensity increases towards the spring, which causes net radiation to become dominant in both sites. Sources of energy contributing to snowmelt in mid-winter both in the open and in the forest are strongly dependent on air temperature. Sensible heat flux is directly proportional to the temperature gradient above the snow surface and net radiation is dominated by the long-wave components, which are functions of radiation source temperatures. As winters in coastal areas of

southern Finland comprise several melt periods and melt intensity is sensitive to the air temperature, a change in the local climate would have a prominent effect on the extent and depth of the snow cover.

Acknowledgements

This study was funded by the Academy of Finland project 'Predicting impacts of land-use changes on catchment hydrological processess' headed by Prof. Pertti Vakkilainen. The authors also received funding from the Land and Water Technology Foundation, the Finnish Cultural Foundation, and the Oskar Öfflund Foundation. The authors are grateful to Mr Pertti Hyvönen and Mr Matti Keto for their help with field instrumentation. Comments of Dr Angela Lundberg, and reviews of Dr Rachel Jordan and an anonymous reviewer improved quality of the paper. Discussions on forest hydrology with Prof. Tuomo Karvonen and Mr Mikko Jauhiainen are acknowledged.

References

Anderson, E.A., 1976. A point energy and mass balance model of a snow cover, NOAA Technical Report NWS 19, 150 pp.

Aston, A.R., 1979. Rainfall interception by eight small trees. J. Hydrol. 42, 383–396.

Brutsaert, W., 1982. Evaporation into the Atmosphere—Theory, History, and Applications. D. Reidel Publishing Company, Dordrecht 299 pp.

Calder, I.R., 1990. Evaporation in the Uplands. Wiley, Chichester.

Choudhury, B.J., Monteith, J.L., 1988. A four-layer model for the heat budget of homogeneous land surfaces. Q. J. R. Meteorol. Soc. 114, 373–398.

Davis, R.E., Hardy, J.P., Ni, W., Woodcock, C., McKenzie, J.C., Jordan, R., Li, X., 1997. Variation of snow cover ablation in the boreal forest—a sensitivity study on the effects of conifer canopy. J. Geophys. Res. 102 (D24), 29389–29395.

Dolman, A.J., 1993. A multiple-source land surface energy balance model for use in general circulation models. Agric. For. Meteorol. 65 (1–2), 21–45.

Førland, E.J., Allerup, P., Dahlström, B., Elomaa, E., Jónsson, T., Madsen, H., Perälä, J., Rissanen, P., Vedin, H., Vejen, F., 1996. Manual for operational correction of nordic precipitation data. 24, DNMI, 66 pp.

Giesbrecht, M.A., Woo, M., 2000. Simulation of snowmelt in a subarctic spruce woodland: 2. Open woodland model. Wat. Resour. Res. 36 (8), 2287–2295.

Harding, R.J., Pomeroy, J.W., 1996. Energy balance of the winter boreal landscape. J. Clim. 9 (11), 2778–2787.

Hardy, J.P., Davis, R.E., Jordan, R., Li, X., Woodcock, C., Ni, W., McKenzie, J.C., 1997. Snow ablation modeling at the stand scale in a boreal jack pine forest. J. Geophys. Res. 102 (D24), 29397–29405.

Hardy, J.P., Davis, R.E., Jordan, R., Ni, W., Woodcock, C.E., 1998. Snow ablation modelling in a mature aspen stand of the boreal forest. Hydrol. Process. 12 (10–11), 1763–1778.

Illangasekare, T.H., Walter Jr., R.J., Meier, M.F., Pfeffer, W.T., 1990. Modeling of meltwater infiltration in subfreezing snow. Wat. Resour. Res. 26 (5), 1001–1012.

Jordan, R., 1991. A one-dimensional temperature model for a snow cover: technical documentation for SNTHERM.89. Special Report 91-16, US Army Cold Regions Research and Engineering Laboratory, Hanover, 49 pp.

Jordan, R., 1992. Estimating turbulent transfer functions for use in energy balance modeling. Internal Report 1107, US Army Cold Regions Research and Engineering Laboratory, Hanover, 13 pp.

Jordan, R.E., Andreas, E.L., Makshtas, A.P., 1999. Heat budget of snow-covered sea ice at North Pole 4. J. Geophys. Res. 104 (C4), 7785–7806.

Karvonen, T., 1988. A model for predicting the effect of drainage on soil moisture, soil temperature and crop yield. Publications of the Laboratory of Hydrology and Water Resources Engineering 1/1988Helsinki University of Technology, Espoo 215 pp.

Koivusalo, H., Heikinheimo, M., Karvonen, T., 2001. Test of a simple two-layer parameterisation to simulate energy balance and temperature of a snowpack. Theor. Appl. Climatol. 70, 65–79.

Kustas, W.P., Rango, A., Uijlenhoet, R., 1994. A simple energy budget algorithm for the snowmelt runoff model. Wat. Resour. Res. 30 (5), 1515–1527.

Kuusisto, E., 1984. Snow Accumulation and Snowmelt in Finland. , Publications of the Water Research Institute 55. National Board of Waters, Helsinki, Finland 149 pp.

Lepistö, A., 1994. Areas contributing to generation of runoff and nitrate leaching as estimated by empirical isotope methods and TOPMODEL. Aqua. Fenn. 24, 103–120.

Lepistö, A., Kivinen, Y., 1997. Effects of climatic change on hydrological patterns of a forested catchment: a physically based modeling approach. Boreal Environ. Res. 2, 19–31.

Link, T., Marks, D., 1999. Distributed simulation of snowcover mass- and energy-balance in the boreal forest. Hydrol. Process. 13 (14–15), 2439–2452.

Lundberg, A., 1993. Evaporation of intercepted snow—review of existing and new measurement methods. J. Hydrol. 151 (2–4), 267–290.

Lundberg, A., 1996. Interception evaporation, processes and measurement techniques. 196 D, Division of Water Resources Engineering, Luleå University of Technology, 24 pp.

Lundberg, A., Halldin, S., 1994. Evaporation of intercepted snow—analysis of governing factors. Wat. Resour. Res. 30 (9), 2587–2598.

Lundberg, A., Calder, I., Harding, R., 1998. Evaporation of intercepted snow—measurement and modelling. J. Hydrol. 206 (3–4), 151–163.

Male, D.H., Granger, R.J., 1981. Snow surface energy exchange. Wat. Resour. Res. 17, 609–627.

Marshall, S., Oglesby, R.J., Maasch, K.A., Bates, G.T., 1999.

Improving climate model representations of snow hydrology. Environ. Model. Software 14, 327–334.

Nakai, Y., Sakamoto, T., Terajima, T., Kitamura, K., Shirai, T., 1999. Energy balance above a boreal coniferous forest: a difference in turbulent fluxes between snow-covered and snow-free canopies. Hydrol. Process. 13 (4), 515–529.

Ohta, T., 1994. A distributed snowmelt prediction model in mountain areas based on an energy balance method. Ann. Glaciol. 19, 107–113.

Pomeroy, J.W., Dion, K., 1996. Winter radiation extinction and reflection in a boreal pine canopy—measurements and modelling. Hydrol. Process. 10 (12), 1591–1608.

Pomeroy, J.W., Parviainen, J., Hedstrom, N., Gray, D.M., 1998. Coupled modelling of forest snow interception and sublimation. Hydrol. Process. 12 (15), 2317–2337.

Price, A.G., Dunne, T., 1976. Energy balance computations of snowmelt in a subarctic area. Wat. Resour. Res. 12, 686–694.

Satterlund, D.R., 1979. An improved equation for estimating longwave radiation from the atmosphere. Wat. Resour. Res. 15, 1643–1650.

Storck, P., 2000. Trees, snow and flooding: an investigation of forest canopy effects on snow accumulation and melt at the plot and watershed scales in the Pacific North West. Water Resources Series, Technical Report No. 161, University of Washington, Seattle, 176 pp.

Tarboton, D.G., Luce, C.H., 1996. Utah Energy Balance Snow Accumulation and Melt Model (UEB), Computer Model Technical Description and Users Guide. Utah Water Research Laboratory and USDA Forest Service Intermountain Research Station 39 pp.

Tarboton, D.G., Chowdhury, T.G., Jackson, T.H., 1995. A spatially distributed energy balance snowmelt model. In: Tonnessen, K.A., Williams, M.W., Tranter, M. (Eds.). Biogeochemistry of Seasonally Snow-Covered Catchments. IUGG Symposium, Boulder, July (1995), 228. IAHS Publications, pp. 141–155.

Troendle, C.A., 1983. The potential for water yield augmentation from forest management in the Rocky Mountain region. Wat. Resour. Bull. 19 (3), 359–373.

Troendle, C.A., King, R.M., 1987. The effect of partial and clearcutting on streamflow at Deadhouse Creek. Colorado J. Hydrol. 90, 145–157.

Tuteja, N.K., Cunnane, C., 1997. Modelling coupled transport of mass and energy into the snowpack—model development, validation and sensitivity analysis. J. Hydrol. 195 (1–4), 232–255.

Vehviläinen, B., 1992. Snow Cover Models in Operational Watershed Forecasting. Publications of Water and Environment Research Institute 11, National Board of Waters and the Environment, Helsinki, 112 pp.

Wigmosta, M.S., Vail, L.W., Lettenmaier, D.P., 1994. A distributed hydrology–vegetation model for complex terrain. Wat. Resour. Res. 30 (6), 1665–1679.

Woo, M., Giesbrecht, M.A., 2000. Simulation of snowmelt in a subarctic spruce woodland: 1. Tree model. Wat. Resour. Res. 36 (8), 2275–2285.